

# Sizing Considerations for EV Dynamic Wireless Charging Systems with Integrated Energy Storage

Donovin D. Lewis, Huangjie Gong, Greg Erhardt<sup>1</sup>, Rong Zeng<sup>2</sup>, Omer Onar<sup>2</sup>,  
Veda Prakash Galigekere<sup>2</sup>, Burak Ozpineci<sup>2</sup>, and Dan M. Ionel

SPARK Laboratory, ECE Department, University of Kentucky, Lexington, KY, USA

<sup>1</sup>Civil Engineering Department, University of Kentucky, Lexington, KY, USA

<sup>2</sup>Power Electronics and Electric Machinery Group, Oak Ridge National Laboratory, Knoxville, TN, USA

donovin.lewis@uky.edu, huangjie.gong@uky.edu, greg.erhardt@uky.edu, zengr@ornl.gov,  
onaroc@ornl.gov, galigekerevn@ornl.gov, burak@ornl.gov, dan.ionel@uky.edu

**Abstract**—Roadways with dynamic wireless charging systems (DWCS) enable charge-sustaining in-motion EV charging, which can reduce charging idle time while increasing range capabilities. Spatially distributed transmitter coils are controlled in response to traffic load that varies significantly minute to minute with high power levels, very short charging time, and low system utilization like wind turbine power. Traffic load estimation and localized analysis may guide effective sizing and topology adoption for feasible and scalable DWCS deployment. DWCS traffic load approximation is reviewed with measured Automated Traffic Recorder (ATR) data and statistical distributions being used to create a synthetic load analyzed using proposed metrics quantifying system utilization over time. Lumped coil section segmentation is compared between second-based distance and spatial density analysis methods, offering 17-27% greater system utilization. A peak load shifting method is proposed for traffic redirection across two tracks with optional BESS integration increasing system utilization by 50-60% depending on time-based and power reserve-based sizing and control.

**Index Terms** – Electric vehicle (EV), dynamic wireless charging, transportation electrification, wireless power transfer, energy storage.

## I. INTRODUCTION

Electric vehicle (EV) deployment has greatly accelerated in part due to rising gas prices, increased energy efficiency, and the potential for significantly reduced emissions. One of the biggest challenges for the widespread adoption of EVs is range anxiety due to limited distributed charging systems and reduced energy density in batteries compared to conventional fuels. Dynamic wireless charging system (DWCS) deployment could play a large part in mitigating range-related anxiety through charge-sustaining operation, supplying power sufficient for continued travel to EVs in motion. Previous studies have found that 200kW systems covering 8-10% of primary roadway at highway speeds can allow charge-sustaining (CS) operation on 99.3% of EV driving cycles [1].

Dynamic wireless charging uses electromagnetic coupling as shown in Fig. 1(a) to charge vehicles in-motion, extending cruising ranges while reducing battery pack capacity requirements and idle charging times [2], [3]. Power output is virtually constant and controlled on the grid-side in response to traffic flow, the number of vehicles at an instant in time, across the roadway and above transmitter coils [4], [5]. The

active charging window and power demand is therefore heavily dependent on vehicle speed and the number and size of transmitter and receiver coils.

A major challenge for DWCS planning is the randomness of traffic density and vehicle speed, which define maximum system power demand. High power output of 200 kW per coil, akin to that of a DC fast charger in price and scale, is desired to maximize the energy transferred to the battery while maintaining reasonable cost. Topology and implementation strategies for DWCS have been explored prior [5], [6] to minimize system interconnections and size while providing for majority of the traffic load. These systems vary in using either a stretched topology, using long tracks with lower efficiency and coupling performance [7], or a lumped topology, where multiple coils are connected either individually or in large groups to power converters [8], [9].

In one example case, employing laboratory demonstrated technology shown in Fig. 1(b) from [10], a typical number,  $n_c$ , of 50 coils of single-lane width and a length,  $L_c$ , of 1.61 meters are connected in a section supplied by a 230kW converter. For a one-mile long single track road with 980 coils, segmentation could create 20 coil sections each with its own converter, adding up to an accumulated rating of 4.6MW. Application on a tightly regulated road with a constant vehicle speed,  $S_v$ , of 60mph and a minimum 2s time difference,  $t_d$ , between vehicles fulfills the condition:  $n_c * L_c \leq S_v * t_d$  similar to that presented in [11].

In this paper, the cross-disciplinary intersection of traffic behavior and DWCS load are explored, metrics are developed to quantify topology effectiveness, and multiple DWCS configurations are proposed to increase power electronic capacity factor. Within the modeled system, it is assumed that 100% of driving of EVs have WPT capability, 1 mile of interstate is covered through DWCS coils, analysis results are location-specific depending on the traffic behavior at that interstate, power is regulated, and cars are travelling at constant (free flow) speed.

## II. TRAFFIC-BASED LOAD MODELING FOR DWCS

Daily load profiles for DWCS are highly dependent on the number and speed of vehicles across the specified roadway.

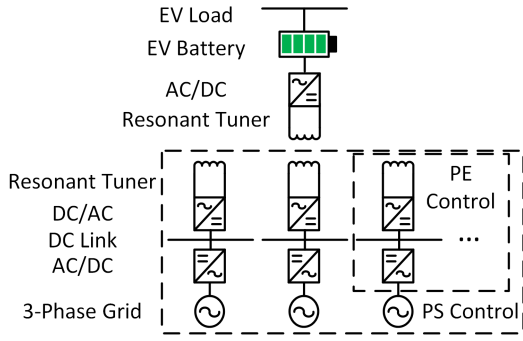


Fig. 1. Schematic for a dynamic wireless charging system (DWCS) with controls at device and aggregated level responding to traffic behavior, and a DWCS laboratory prototype considered as part of the current study.

TABLE I  
PARAMETERS FOR DWCS MODELING

Parameters	Value
Power Draw per Coil	230 kW
Charging Efficiency	90%
Length of Transmitter Coil	1.73 meters
Length of Charging Track	1 mile
AADT	55,187
Vehicle Speed	70 ± 5 mph
Initial BESS SOC	35%
Minimum BESS SOC	20%

Previous DWCS impact studies assuming varying penetration of WPT enabled EVs have used sensing data including GPS stamped driving cycles at 1 second resolution [3], weigh-in-motion data at 0.1 seconds [6], and mesoscopic traffic simulation at a 5 second resolution [12]. When lacking high-resolution traffic data, we can generate an approximation of the traffic load by stochastically interpolating the time of vehicle arrival and approximating constant vehicle speed as performed prior in [5], [13] at a minutely resolution and [12] at a second resolution.

Sub-hourly traffic data, like in Fig. 4, within this study is estimated using annual average daily traffic (AADT) provided through the Kentucky Transportation Cabinet's Interactive Statewide Traffic Counts Map [14] and an hourly traffic distribution (HTD) from 900+ days of hourly Automated Traffic Recorder (ATR) traffic counts on the target highway, I-75 near Bowling Green, KY. For comparison, we plotted our data derived HTD against the data used in [5] from the 2009 US National Household Travel Survey (NHTS) [15] in Fig. 3. Our experimental data showcases an afternoon peak compared to the 2009 NHTS data akin to long-distance roadway traffic, leading to the introduction of the hybrid split-track system proposed for improved system utilization.

$$V_a(h) = \frac{N_h(h)}{\sum_{h=0}^{23} N_h} * AADT = P(h) * AADT \quad (1)$$

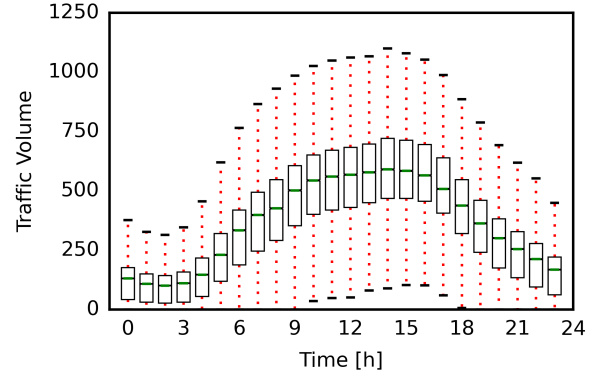


Fig. 2. Box and whisker plot for the experimental ATR data from an example interstate highway in traffic volume for all 900+ days of hourly traffic data.

$$V_a(n) = \frac{e^{-\lambda * t} * (\lambda * t)^n}{n!} \text{ where } \lambda = V_a(h) * \Delta(t) \quad (2)$$

$$S_v(V) = \frac{1}{\sigma \sqrt{2\pi}} * e^{-\frac{1}{2}(\frac{V-\lambda}{\sigma})^2} \quad (3)$$

Interpolation of sub-hourly vehicle arrival is described by (1), (2), and (3) with (1) estimating the number of vehicles per hour on the roadway ( $V_a(h)$ ) as a product of the AADT and the percentage of cars per day expected to arrive on the road at that hour ( $P(h)$ ). A Poisson distribution was used to approximate the number of vehicles arriving at every minute ( $V_a(n)$ ) using the hourly vehicle count as the mean,  $\lambda$  as shown in (2). For each vehicle, a normal distribution is used with the speed limit as the mean,  $\lambda$ , and assuming a standard deviation,  $\sigma$ , to sample a constant speed per vehicle ( $S_v(V)$ ) on the roadway in (3). For every minute across the 24 hour period, the number of vehicles currently on the track are counted based on their time of arrival and speed and multiplied by the constant 230 kW load per coil to generate an aggregate load.

A box and whisker plot describing day to day traffic

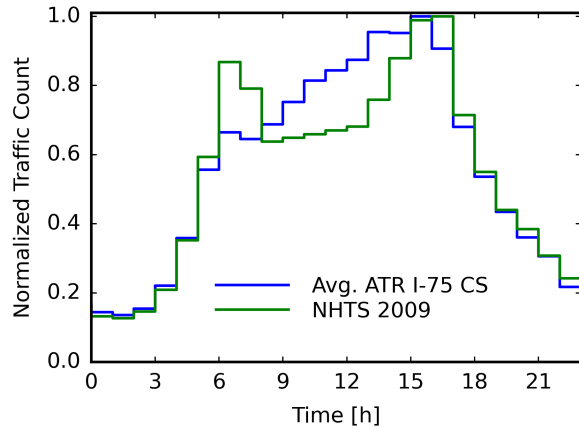


Fig. 3. Hourly traffic distribution based on experimental ATR data from the KY I-75 case study considered and the 2009 NHTS data with per unit bases of 2.3 and 9.1 thousand vehicles, respectively.

variation can be found in Fig. 2 with much of the variation occurring between hours 6 and 18. For the following DWCS configuration analysis, the load was divided by 3 to create an average traffic per lane and each lane and the associated power electronics are defined as tracks. An example track load curve from the Bowling Green ATR data is shown in Fig. 4, using the parameters described in Table I, and a confidence interval capturing 95% of daily travel created using stochastic methods of synthetic data generation. Daily track load profiles can be used as a basis of comparison for segmentation topologies and the impact of traffic regulation modification for system capacity factor and power ripple.

The sections of DWCS consists of two primary parties: device-level control of individual transmitters to maximize efficiency depending on electromagnetic characteristics, and an aggregator that coordinates response to the traffic load, focusing on minimizing costs and maximizing customers depending on the expected traffic flow. Within this co-dependent system, aggregate control of coils separate from the power electronic control could be used to adjust power draw and system utilization based on traffic characteristics (Fig. 1(a)). In the quintessential example, a traffic jam, aggregate control of coils, assuming SOC is transmitted alongside payment info and vehicle position, could be handed with the goal of offsetting the very low electrical energy required for low speed movement. Assuming toggleable coils and precise vehicle location sensing, handing switching control to the power systems control enables maximum flexibility for outlier traffic scenarios while maintaining feasible sizing.

### III. ALTERNATIVE CONFIGURATION OF DWCS FOR INCREASED POWER ELECTRONIC CAPACITY FACTOR

For feasible DWCS deployment, devices are constrained by their power rating, which greatly impacts overall system cost [4]. Insights gained through traffic modeling enable the development of alternative traffic and power electronic configurations to improve system utilization estimated using (4).

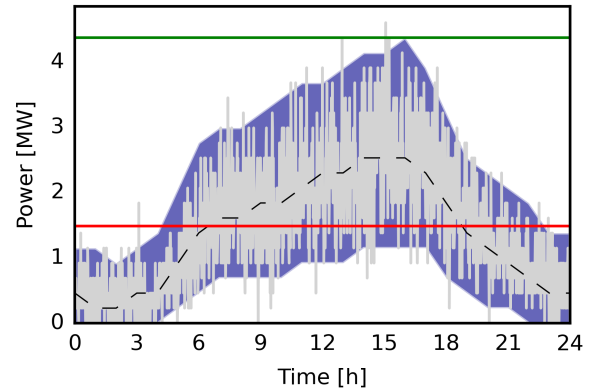


Fig. 4. Daily power demand for a 1 mile road equipped with DWCS coils and 95% confidence interval based on an hourly traffic distribution derived from example ATR data assuming 100% EV and wireless charging capability penetration.

System utilization or capacity factor within the current study, summarized in (4), is defined as the average power output divided by the system's maximum rating for a track with higher utilization indicating greater device utilization within the system.

Compared to the heavily regulated case study briefly described in the introduction, the other extreme would be a highway with minimal user behavior regulation and considering one track, as shown in Fig. 7. Based on these results, a total accumulated system rating of 4.37 MW, shown in green, for 100% vehicle dynamic wireless charging along 1 mile, may provide with a very high level of confidence the typical required charging power for EVs. The average power for the load curve of Fig. 7, shown in red, is 1.49 MW and hence a system utilization of 41% which is comparable to other power electronic applications for largely variable resources, such as wind turbines.

Within lumped track systems, transmitter coil segmentation, like that shown in Fig. 5, can be deployed to improve overall system utilization by connecting multiple coils to a single converter but risks multiple cars travelling over the same section at a time, requiring advanced device controllability [11], [16]. For the segmentation of distributed lumped coils, two models for segmentation are proposed and simulated, one using an approximate vehicle length of 7.62 meters similar to [16], typically used in civil engineering modeling, and another using the 2 second safe distance between vehicles, like in [11], to evaluate system utilization improvement for both:

$$CF = \frac{\frac{1}{T} \int_0^T P(t) dt}{P_{max}} \quad (4)$$

$$k = \frac{V_{num}}{\frac{T_L}{V_L}}, C_{act} = \frac{k}{C_L}, C_{sec} = \frac{C_{num}}{max(C_{act})} \quad (5)$$

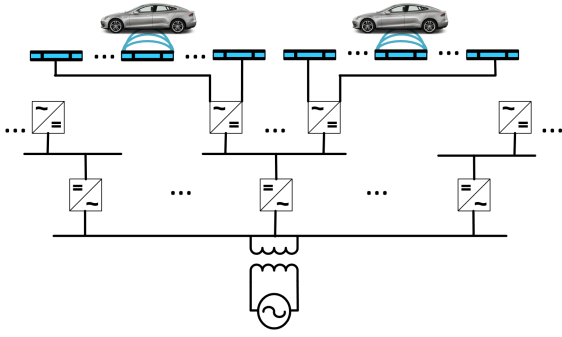


Fig. 5. Example segmented track with a shared grid-connecting transformer, shared DC bus between HF converters, and coil section segmentation, which can increase system utilization by 17-27%.

$$PE_{act} = \frac{C_{act}}{\frac{C_{num}}{C_{sec}}}. \quad (6)$$

Spatial density analysis was applied to a lumped coil track setup, as described in (5) and (6) where  $C$  stands for coil,  $k$  for density,  $T$  for track,  $V$  for vehicle,  $L$  for length,  $_{act}$  is the current active number, and  $_{sec}$  the number of sections. Spatial density of the roadway, defined in (5) is determined as the quotient of the number of cars on the track across the day by the amount of spots available for one car each assuming a defined vehicle length. The roadway coil density and the spatial density, in (5) is then used to determine the number of active coils at any time whose maximum can be used to determine the number of coils per coil section in (5). Overall system utilization can then be estimated through (6) using section on-time depending on the traffic density over the course of the day.

The lumped coil track assuming a 7.62 meter vehicle resulted in a maximum of 10 coils per section with a maximum of 89 coils activated per minute on the roadway for an average system utilization of 30.6% compared to an average 3% utilization with individual coil-converter connections. The quotient of roadway length by the length of time necessary to sustain a minimum distance between cars can also be used to determine the number of sections. Applying this methodology with the Kentucky standard 2 second minimum between cars results in 25 coil sections with 38 coils per section and a maximum of 20 coils activated per minute for an average system utilization of 17%. Localized maximum system utilization can also be quantified as the ratio between cars on the roadway and the maximum cars at any point in time, enabling coil length and sectioning optimization per location, with a maximum utilization of 32.3% at the Bowling Green roadway section.

#### IV. BESS AND DWCS INTEGRATION FOR REDUCED PEAK POWER DEMAND

To improve upon system utilization, energy storage systems may be interconnected to the DC link to shift demand across

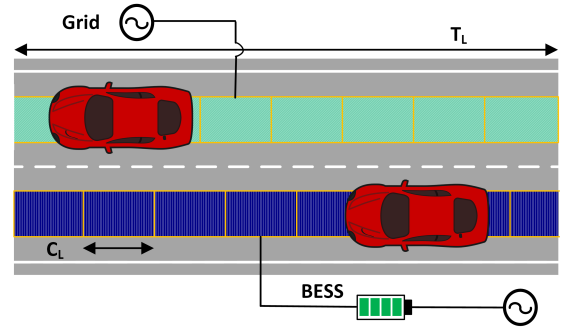


Fig. 6. Split-track hybrid DWCS configuration with a grid-connected BESS charging during off-hours and discharging to power one track of the roadway during peak periods to shift peak power consumption.

time and reduce peak power system demand. Two methods are proposed for the sizing and control of energy storage systems to meet the majority of daily demand by sizing dependent on the 95% confidence interval. Within peak hours, traffic for two tracks (Fig. 8(a)) is split to increase overall system utilization, one with majority of the both track's load and another to overflow during peak traffic loading with an optional battery energy storage system (BESS), like in [17] as depicted in Fig. 6. The resulting system capacity factors for both methods are compared to the conventional two track case in Table II.

Assumptions for Li-Ion BESS simulation include a starting SOC of 35%, a depth of discharge,  $DOD$ , of 80%, and no self-discharge or round-trip efficiency loss for best case scenario analysis with balanced traffic between tracks prior to redirection. Depending on the region of installation, geographically distributed energy storage and production, like pumped hydro or concentrated solar power thermal storage, may be more cost feasible than the utilization of Li-Ion BESS as assumed within this study. For both methods, the BESS charging power is sized such that the power dispersed over allocated charging hours meets the energy necessary for the diverted traffic,  $E_{ES}$ , with BESS capacity,  $E_{cap}$ , sized using the demanded energy as shown in (7).

$$\min(E_{cap}) = \frac{\max(E_{ES}) - \min(E_{ES})}{DOD} \quad (7)$$

The first method, depicted in Fig. 8(b), focuses upon halving demand on track one (T1) during peak time periods across the day through track two (T2) with an optional BESS. Between periods of reduced load, for example, the BESS system is charged using the power electronics for T2 while T1 charges cars that pass over it before T2's BESS discharges during the peak to effectively shift load (Fig. 7(a)). An example charging and discharging application is shown in Fig. 7(b) with dynamically allocated BESS charging power and maintaining pre-defined SOC limitations, plotted in the dashed red line. The results of two cases using this method are listed in Table II with increased time periods reducing T1 utilization and increases T2 utilization but the introduction of BESS increases track two capacity factor by as much as 60%.

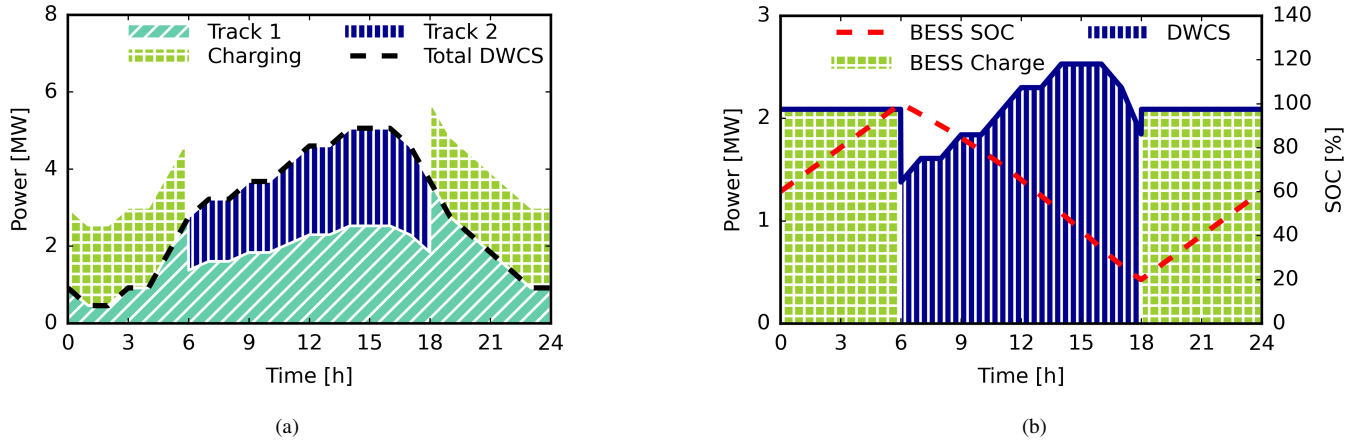


Fig. 7. Power profile for a hybrid DWCS configuration in (a) a stacked two track hybrid DWCS arrangement with traffic redirected towards both tracks for charging during peak loading periods between 6:00 and 18:00 and (b) the input/output power into the second track within the same time period with an integrated BESS system alongside the dynamic BESS SOC.

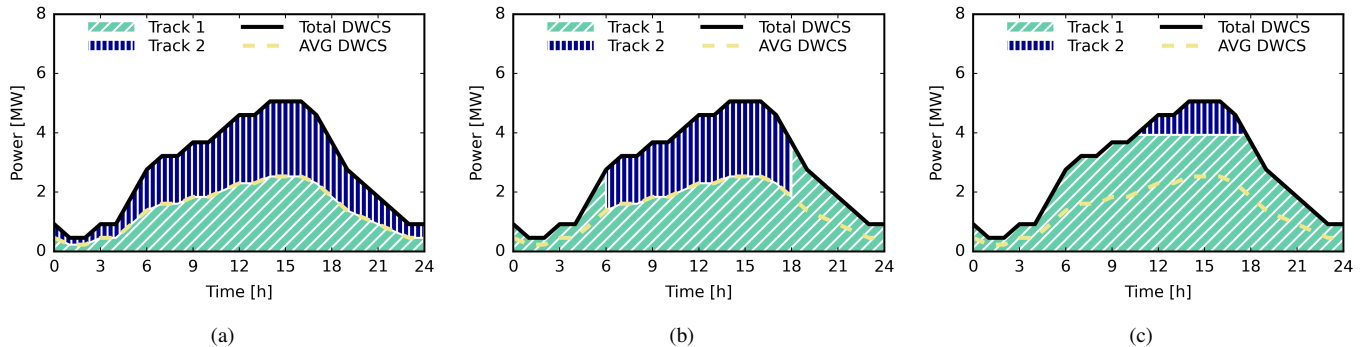


Fig. 8. Power profiles for a hybrid-split track configuration with optional BESS storage: (a) a conventional two-track traffic load traffic, (b) a time-based split across two tracks splitting one track's power between 6 and 18:00 hours, and (c) a reserve-power based peak reduction as a percentage of the maximum power output for both tracks. System utilization for the second track increases by 50-60% due to BESS availability.

A second method, shown in Fig. 8(c), was proposed and simulated with a power reserve that can be used for system redundancy or shifting between tracks 1 and 2, similar to that performed in [18]. A percentage of the maximum power for combined track demand is shifted to the second track with a BESS to reduce peak demand and improve system utilization on T1. If the goal is meant for redundancy, track one's performance doesn't change while system stability is increased. If the goal is meant to instead reserve power and use the second track, the maximum power on T1 shifts, increasing capacity factor in T1 and T2 with and without BESS. Two reserved redirection case results are summarized in Table II with increased reservation percentage increasing T1 and T2 capacity factor with the introduction of BESS doubling track two capacity factor.

The results of both methods is highly dependent on the characteristic localized traffic behavior resulting in non-linear variation in track one and track two capacity factor. Additionally, the integration of BESS akin to those mentioned in [12], [19], enables greater capability for the integration of renewable

energy generation and power smoothing to mitigate the effect of traffic load variation on the larger system.

## V. CONCLUSION

In this paper, measured traffic data was used for the modeling, analysis, and sizing of dynamic wireless charging systems for a roadway using localized measured automated traffic recorder data and sampled statistical distributions. System device sizing is suggested based on a 90-95% confidence interval for traffic load aggregated from multiple instances of synthetically generated traffic. A metric for overall system utilization is introduced as a ratio of local average and the rated power output for the system to inform scalability-focused decisions.

Traffic load spatial density analysis was performed for system segmentation purposes based on the minimum distance between cars, length of the track, and number of coils on the roadway. Methods of lumped coil track segmentation are proposed for instantaneous spatial distribution of vehicles and the distance between vehicles with system capacity factor increasing by 27% or 17% respectively, assuming a single

TABLE II  
IMPACT OF ALTERNATIVE HYBRID SPLIT-TRACK CONFIGURATION ON SYSTEM UTILIZATION.

Case		Capacity Factor [%]			BESS	BESS
		T1	T2	w/o BESS	T2 w. BESS	Capacity [MWh]
Conventional		41	24		N/A	N/A
Time Redirection	12-18:00	51	14		47	17.8
	6-18:00	41	24		83	31.3
Reserved Redirection	10%	66	20		40	6.8
	30%	74	28		57	17.2

car per section. Two methods of load shifting were proposed, modeled, and analyzed to increase power electronic utilization through traffic redirection. The first method, a time-based split of load on two tracks, resulted in increased system capacity factor on the redirected track by 60% with integrated BESS systems. The second method based on reservation of power from the maximum of both tracks, increased the system utilization of both tracks and can double the capacity factor with an added BESS. The cross-disciplinary development of DWCS configurations can guide the adoption of feasible, scalable deployment on real roadways and is reliant on reliable traffic modeling and aggregate control alongside informed sizing of coil-converter configurations.

#### ACKNOWLEDGMENT

This work was supported by the NSF Graduate Research Fellowship under Grant No. 1839289. Any findings and conclusions expressed herein are those of the authors and do not necessarily reflect the views of the NSF. The support of the University of Kentucky through the Otis A. Singletary Graduate Research Fellowship is also gratefully acknowledged.

#### REFERENCES

- [1] V. Galigekere and B. Ozpineci, "High Power and Dynamic Wireless Charging of Electric Vehicles (EVs)," Online, Jun. 2021. [Online]. Available: [https://www.energy.gov/sites/default/files/2021-06/elt197\\_galigekere\\_2021\\_o\\_5-18\\_505pm\\_LR\\_TM.pdf](https://www.energy.gov/sites/default/files/2021-06/elt197_galigekere_2021_o_5-18_505pm_LR_TM.pdf)
- [2] H. Feng, R. Tavakoli, O. C. Onar, and Z. Pantic, "Advances in high-power wireless charging systems: Overview and design considerations," *IEEE Transactions on Transportation Electrification*, vol. 6, no. 3, pp. 886–919, 2020.
- [3] B. J. Limb, T. H. Bradley, B. Crabb, R. Zane, C. McGinty, and J. C. Quinn, "Economic and environmental feasibility, architecture optimization, and grid impact of dynamic charging of electric vehicles using wireless power transfer," in *6th Hybrid and Electric Vehicles Conference (HEVC 2016)*, 2016, pp. 1–6.
- [4] A. Foote, O. C. Onar, S. Debnath, M. Chinthavali, B. Ozpineci, and D. E. Smith, "Optimal sizing of a dynamic wireless power transfer system for highway applications," in *2018 IEEE Transportation Electrification Conference and Expo (ITEC)*, 2018, pp. 1–6.
- [5] R. Zeng, V. P. Galigekere, O. C. Onar, and B. Ozpineci, "Grid integration and impact analysis of high-power dynamic wireless charging system in distribution network," *IEEE Access*, vol. 9, pp. 6746–6755, 2021.
- [6] D. Haddad, T. Konstantinou, A. Prasad, Z. Hua, D. Aliprantis, K. Gkritza, and S. Pekarek, "Data-driven design and assessment of dynamic wireless charging systems," in *2019 IEEE PELS Workshop on Emerging Technologies: Wireless Power Transfer (WoW)*, 2019, pp. 59–64.
- [7] L. Tan, W. Zhao, M. Ju, H. Liu, and X. Huang, "Research on an ev dynamic wireless charging control method adapting to speed change," *Energies*, vol. 12, no. 11, 2019. [Online]. Available: <https://www.mdpi.com/1996-1073/12/11/2214>
- [8] C. Panchal, S. Stegen, and J. Lu, "Review of static and dynamic wireless electric vehicle charging system," *Engineering Science and Technology, an International Journal*, vol. 21, no. 5, pp. 922–937, 2018. [Online]. Available: <https://www.sciencedirect.com/science/article/pii/S221509861830154X>
- [9] D. D. Marco, A. Dolara, and M. Longo, "A review on dynamic wireless charging systems," in *2019 IEEE Milan PowerTech*, 2019, pp. 1–5.
- [10] "Going wireless for better vehicle charging | ORNL." [Online]. Available: <https://www.ornl.gov/blog/going-wireless-better-vehicle-charging>
- [11] D. Naberezhnykh, N. Reed, F. Ognissanto, T. Theodoropoulos, and H. Bludszweit, "Operational requirements for dynamic wireless power transfer systems for electric vehicles," in *2014 IEEE International Electric Vehicle Conference (IEVC)*, 2014, pp. 1–8.
- [12] T. Theodoropoulos, A. Amditis, J. Sallan, H. Bludszweit, B. Berseneff, P. Guglielmi, and F. Deflorio, "Impact of dynamic EV wireless charging on the grid," in *2014 IEEE International Electric Vehicle Conference (IEVC)*. Florence: IEEE, Dec. 2014, pp. 1–7. [Online]. Available: <https://ieeexplore.ieee.org/document/7056234/>
- [13] O. Hafez and K. Bhattacharya, "Integrating EV Charging Stations as Smart Loads for Demand Response Provisions in Distribution Systems," *IEEE Transactions on Smart Grid*, vol. 9, no. 2, pp. 1096–1106, Mar. 2018. [Online]. Available: <https://ieeexplore.ieee.org/document/7485859/>
- [14] "Traffic Counts," publisher: Kentucky Transportation Cabinet. [Online]. Available: <https://maps.kytc.ky.gov/trafficcounts/>
- [15] "Our Nation's Highways: 2011," Nov. 2014, publisher: U.S. Department of Transportation. [Online]. Available: <https://www.fhwa.dot.gov/policyinformation/pubs/hf/pl11028/chapter4.cfm>
- [16] L. Tan, W. Zhao, H. Liu, J. Li, and X. Huang, "Design and optimization of ground-side power transmitting coil parameters for ev dynamic wireless charging system," *IEEE Access*, vol. 8, pp. 74 595–74 604, 2020.
- [17] O. C. Onar, G.-J. Su, E. Asa, J. Pries, V. Galigekere, L. Seiber, C. White, R. Wiles, and J. Wilkins, "20-kw bi-directional wireless power transfer system with energy storage system connectivity," in *2020 IEEE Applied Power Electronics Conference and Exposition (APEC)*, 2020, pp. 3208–3214.
- [18] H. Gong, V. Rallabandi, D. M. Ionel, D. Colliver, S. Duerr, and C. Ababei, "Net zero energy houses with dispatchable solar pv power supported by electric water heater and battery energy storage," in *2018 IEEE Energy Conversion Congress and Exposition (ECCE)*, 2018, pp. 2498–2503.
- [19] R. Zeng, V. Galigekere, O. Onar, and B. Ozpineci, "Optimized renewable energy integration for ev high-power dynamic wireless charging systems," in *2021 IEEE Power Energy Society Innovative Smart Grid Technologies Conference (ISGT)*, 2021, pp. 1–5.